

# Conditional transgenic suppression of M channels in mouse brain reveals functions in neuronal excitability, resonance and behavior

H Christian Peters<sup>1,3</sup>, Hua Hu<sup>2,3</sup>, Olaf Pongs<sup>1</sup>, Johan F Storm<sup>2</sup> & Dirk Isbrandt<sup>1</sup>

**In humans, mutations in the KCNQ2 or KCNQ3 potassium-channel genes are associated with an inherited epilepsy syndrome. We have studied the contribution of KCNQ/M-channels to the control of neuronal excitability by using transgenic mice that conditionally express dominant-negative KCNQ2 subunits in brain. We show that suppression of the neuronal M current in mice is associated with spontaneous seizures, behavioral hyperactivity and morphological changes in the hippocampus. Restriction of transgene expression to defined developmental periods revealed that M-channel activity is critical to the development of normal hippocampal morphology during the first postnatal weeks. Suppression of the M current after this critical period resulted in mice with signs of increased neuronal excitability and deficits in hippocampus-dependent spatial memory. M-current-deficient hippocampal CA1 pyramidal neurons showed increased excitability, reduced spike-frequency adaptation, attenuated medium afterhyperpolarization and reduced intrinsic subthreshold theta resonance. M channels are thus critical determinants of cellular and neuronal network excitability, postnatal brain development and cognitive performance.**

M channels are voltage-gated K<sup>+</sup> channels that underlie the non-inactivating M current ( $I_M$ ) in neurons<sup>1,2</sup>. These channels are of particular interest because they activate at membrane potentials that are more negative than the action-potential threshold and at which few other ion channels are active. Therefore, they may exert pivotal control over neuronal excitability and response patterns<sup>1–4</sup>. This idea is supported by the finding that mutations in the human KCNQ2 and KCNQ3 genes, which are generally believed to encode the main M-channel subunits, cause a dominantly inherited form of human generalized epilepsy called benign familial neonatal convulsions (BFNC)<sup>5</sup>. The BFNC phenotype is characterized by frequent seizures starting in the first week of life. In most cases, the seizures spontaneously disappear within weeks. Although BFNC is generally considered to be a benign epilepsy syndrome, the risk of recurring seizures in adolescence or adulthood is approximately 10–16%, and there are some reports of unfavorable outcomes, notably epileptic encephalopathy or mental retardation<sup>6–8</sup>. In addition to the BFNC phenotype, a family carrying a KCNQ2 mutation also has myokymia, suggesting a potential role for KCNQ2 in motor-neuron or motor-axon function<sup>9</sup>.

The M current was first observed in frog sympathetic ganglia, in which it can be suppressed by muscarinic acetylcholine-receptor activation (hence its name  $I_M$ )<sup>1</sup>. Subsequently, M currents were recorded in mammalian brain neurons, including pyramidal cells of the hippocampus, where M channels are modulated by several neurotransmitters and neuromodulators<sup>3,10</sup>. Several lines of evidence indicate that certain members of the KCNQ gene family encode M-channel subunits that may form homo- or heteromeric M channels<sup>5</sup>. Heteromeric KCNQ2/KCNQ3 channels studied in *in vitro* expression systems have electrophysiological

and pharmacological properties characteristic of M channels<sup>11,12</sup>. In rat sympathetic ganglia, native M channels seem to be composed largely of KCNQ2/KCNQ3 subunits<sup>13</sup>, and these two subunits can be co-immunoprecipitated from human brain lysates<sup>14</sup>. M channels in the mammalian brain may also contain KCNQ5 subunits<sup>15</sup>. Immunohistochemical studies show overlapping KCNQ2 and KCNQ3 protein-expression patterns. This includes co-localization on both the somata and the dendrites of pyramidal and polymorphic neurons in the hippocampus and cerebral cortex, and co-localization on the somata of parvalbumin-positive hippocampal interneurons<sup>16</sup>. KCNQ2/KCNQ3 subunits are also detected in axon initial segments and in central and peripheral axons<sup>16,17</sup>.

M-channel activity is thought to mediate neuronal excitability control and early spike-frequency adaptation<sup>1,2,18,19</sup>, and to generate afterhyperpolarizations of medium duration (mAHPs) during and after repetitive neuronal discharge<sup>4,18</sup>. Thus, M-channel activity tends to stabilize the membrane potential, thereby preventing spiking. Accordingly, attenuation of M-channel activity through activation of G-protein-coupled receptors may enhance neuronal responses to excitatory input<sup>2,10,18,20</sup>. However, the exact function of M channels in the brain—in particular their functions in animal behavior—as well as their roles in the development of epilepsy are not well understood.

To examine the cellular, network and behavioral consequences of M-channel deficiency, we suppressed M currents in the mouse brain. Because genetic KCNQ2 gene deletions are lethal<sup>21,22</sup>, we generated mice expressing a KCNQ2 subunit with a dominant-negative pore mutation that can suppress M-channel activity by co-assembling with native KCNQ subunits. By using the Tet-Off system<sup>23</sup> and the prion-protein

<sup>1</sup>Institut für Neuronale Signalverarbeitung, Zentrum für Molekulare Neurobiologie Hamburg, Martinistrasse 52, 20246 Hamburg, Germany. <sup>2</sup>Department of Physiology, Institute of Basal Medical Sciences, and Centre for Molecular Biology and Neuroscience, University of Oslo, PB 1103, Blindern, N-0317 Oslo, Norway. <sup>3</sup>These authors contributed equally to this work. Correspondence should be addressed to D.I. (isbrandt@uni-hamburg.de) or J.F.S. (j.f.storm@medisin.uio.no).

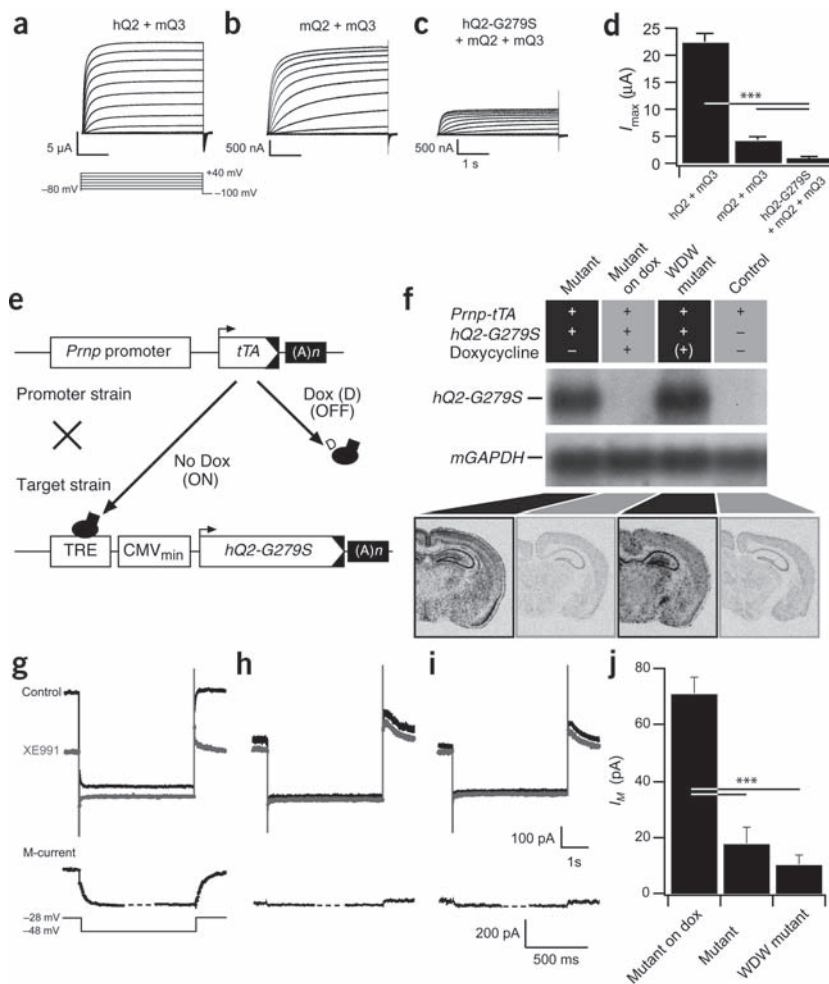


**Figure 1** Generation of  $I_M$ -deficient transgenic mice. (a–c) Two-electrode voltage-clamp recordings from *X. laevis* oocytes injected with equimolar ratios of complementary RNA encoding hKCNQ2 (hQ2) and mKCNQ3 (mQ3) (a), mKCNQ2 (mQ2) and mKCNQ3 (b), and hQ2-G279S, mKCNQ2 and mKCNQ3 (c). (d) Measurements at +40 mV demonstrated a dominant-negative effect of hQ2-G279S. (e) Schematic illustration of the Tet-Off expression system used to generate double-transgenic mice with doxycycline-regulated transgene expression in brain. (f) Doxycycline and genotype-dependent transgene expression in brain was tested in northern blot and *in situ* hybridization experiments using hKCNQ2-specific radiolabeled probes. Animal group designations including genotype and doxycycline treatment regimes are given on top of each lane. For control, the northern blot was probed with a mouse glyceraldehyde-3-phosphate dehydrogenase (mGAPDH) probe. (g–i) Representative current traces of voltage-clamp recordings from CA1 pyramidal neurons in acute slice preparations from male mutant-on-dox (g;  $n = 11$  cells; two mice), mutant (h;  $n = 16$ ; six mice), and WDW mutant (i;  $n = 5$ ; two mice) mice. The upper panel shows the overlay of currents evoked by the protocol shown in g in the absence (black) or presence (gray) of 10  $\mu$ M XE991 (scale as indicated in the inset of i). To illustrate the kinetic components of M-current relaxation and activation, the corresponding difference current (that is,  $I_M$ ) is shown in an expanded scale below each current trace. (j) Summary statistics from experiments shown in g–i reveal attenuated  $I_M$  amplitudes in mutants and WDW mutants. Error bars, s.e.m. \*\*\*,  $P < 0.001$  (*t*-test).

promoter<sup>24</sup>, we gained temporal control over transgene expression and restricted it to the nervous system. This strategy yielded viable M-current-deficient mice. Depending on when during development the transgene was expressed, the mice showed epilepsy, behavioral hyperactivity, cognitive deficits and/or changes in brain morphology. M-channel-deficient mice showed marked electrophysiological changes in their hippocampal CA1 pyramidal neurons: substantially increased excitability, reduced spike-frequency adaptation, attenuated afterhyperpolarizations (mAHPs) and reduced intrinsic subthreshold theta resonance. Furthermore, these mice had markedly impaired spatial memory in the Morris water maze. Our results support the notion that M channels are critical determinants of cellular and neuronal network excitability, and that attenuation of the M current has a profound effect on behavior and cognitive performance.

## RESULTS

### Generation of M-channel-deficient mice

We generated double-transgenic mouse lines that allowed us to suppress M-channel activity in a neuron-specific and doxycycline-dependent manner. The double-transgenic mice expressed the tetracycline-sensitive transactivator (tTA; Tet-Off system)<sup>23</sup> under the control of the prion protein promoter (Prnp)<sup>24</sup>, and a hKCNQ2 pore mutant construct with known dominant-negative properties (hQ2-G279S)<sup>25</sup> fused to a tetracycline-responsive element (TRE; Fig. 1)<sup>23</sup>. We used the human KCNQ2 ortholog to facilitate the detection of transgene expression. Before generating the transgenic mice, we tested the capacity of

hQ2-G279S to attenuate mouse KCNQ2/KCNQ3-mediated currents in an *in vitro* expression system. When co-expressed with mouse KCNQ subunits, hQ2-G279S strongly attenuated the currents mediated by murine KCNQ2/KCNQ3 channels ( $22.5 \pm 2.8 \mu$ A (mean  $\pm$  s.e.m.) for hQ2/mQ3,  $n = 9$ ;  $4.3 \pm 1.7 \mu$ A for mQ2/mQ3,  $n = 5$  and  $1.1 \pm 0.6 \mu$ A for hQ2-G279S/mQ2/mQ3,  $n = 10$ ; Fig. 1). hQ2-G279S was therefore used as a dominant-negative transgene.

The double-transgenic mice that expressed the transgene throughout their life ('mutants') were viable and had a normal appearance at birth. They expressed hQ2-G279S mRNA, as shown by northern blot analysis of whole-brain RNA from mutants (Fig. 1). Neither the doxycycline-fed double-transgenic mice ('mutants on dox') nor the mice carrying only the Prnp-tTA transgene ('controls') expressed detectable levels of hQ2-G279S mRNA (Fig. 1). *In situ* hybridization (ISH) experiments (Fig. 1 and Supplementary Fig. 1 online) showed expression of KCNQ2-G279S mRNA in the cerebral cortex, hippocampus (for example, in the dentate gyrus and in the CA1 and CA3 pyramidal and dendritic-cell layers), striatum and cerebellum of adult mutant brains ( $n = 7$ ; five males, two females). In agreement with northern blot results, only background ISH signals were seen in brain slices from mutants on dox ( $n = 4$ ) and controls ( $n = 6$ ; Fig. 1). Transgene-expressing neurons from male and female mutants showed comparable ISH signal intensities (Supplementary Fig. 1 online). Unlike tissue sections from males, those from female mutant mice showed a mosaic pattern of transgene expression (Supplementary Fig. 1 online). We observed X-chromosomal inheritance of the hQ2-G279S transgene; random X-chromosomal inactivation in

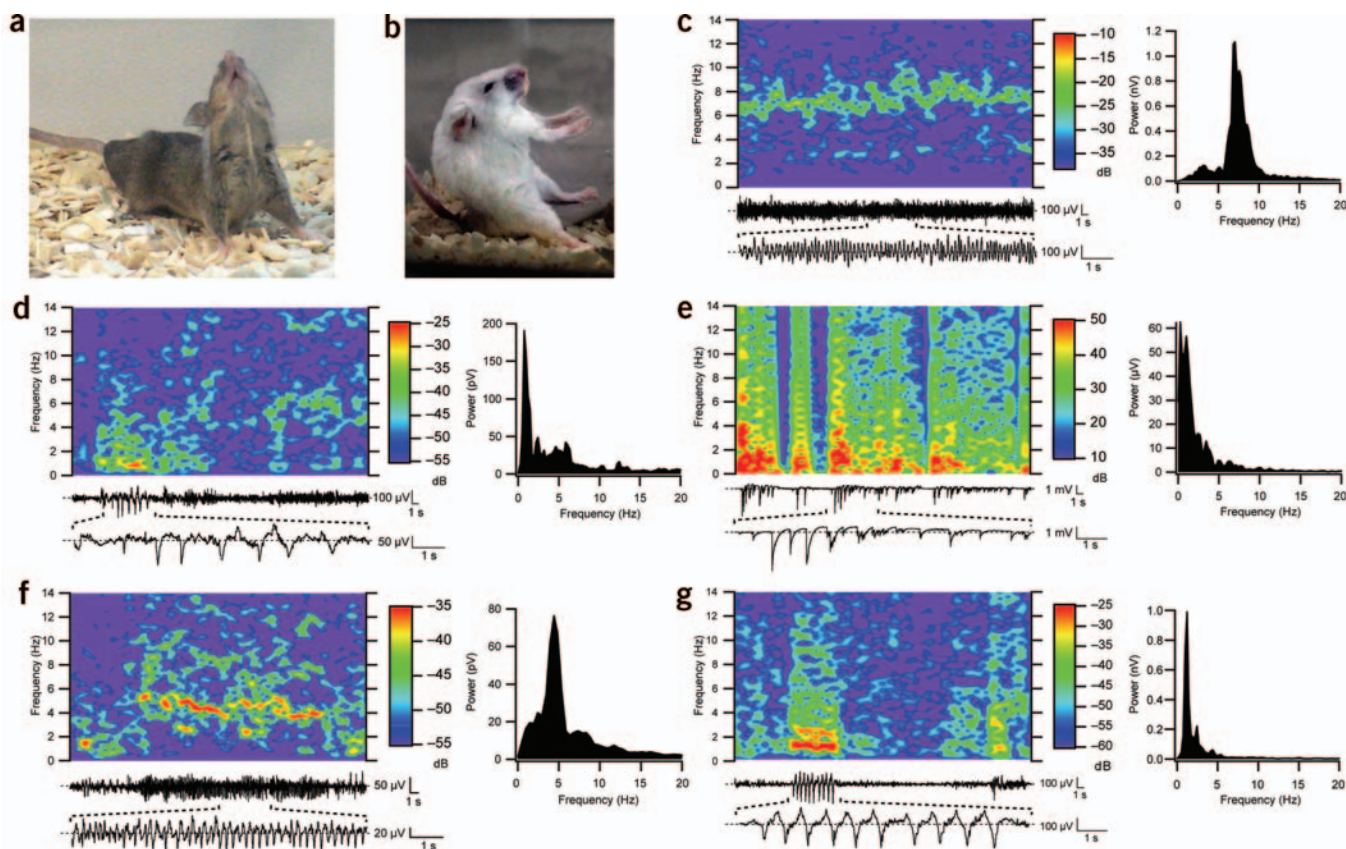


**Figure 2** Spontaneous epileptiform activity in  $I_M$ -deficient mice. **(a,b)** Illustrations of postures during spontaneous partial **(a)** or generalized tonic-clonic **(b)** seizures as observed for male mutants only. **(c–g)** ECoG analysis. Examples of telemetric recordings obtained from undisturbed, freely moving male mice in their home cages (controls  $n = 11$ , mutants  $n = 8$ , WDW mutants  $n = 7$ ). Each panel shows a color-coded power spectrum and the corresponding trace with a duration of 60 s (digitally filtered: low-cut 0.3 Hz and high-cut 30 Hz). A 10-s-long selected epoch of this trace is shown below at an expanded time and amplitude scale. The right part of each panel shows the frequency components of the 60-s trace calculated by conventional fast Fourier transformation (FFT). **(c)** Original ECoG activity recorded from a control animal. Note predominant activity at 7–10 Hz. **(d)** ECoG activity recorded from a mutant showing slow sharp wave activity during a partial seizure involving the left forelimb (see **Supplementary Video 3** online). FFT analysis reveals wideband activity with a peak at about 1 Hz. **(e)** Original trace recorded from a mutant with spontaneous high-voltage spike wave-like complexes. The color-coded power spectrum and FFT of this trace indicate dominant frequencies between 0.5–2.0 Hz. **(f)** Highly synchronous spike activity at frequencies around 4 Hz recorded from a WDW mutant without behavioral accompaniment. Reversal of spike polarity appears to be present at the end of the 60-s trace. **(g)** ECoG recordings from a male WDW mutant with slow spike-and-wave activity during a partial seizure involving the head. The color-coded power spectrum and FFT of this trace reveal dominant frequencies around 1 Hz.

female neurons was therefore the likely cause of the observed mosaicism in hippocampal sections from female mice.

To test whether hQ2-G279S expression in mutant neurons attenuated M-channel activity, we recorded the M current ( $I_M$ ) by whole-cell voltage clamp from CA1 pyramidal cells in acute brain slices from male mutants and mutants on dox. The  $I_M$  amplitude was measured as the amplitude of the characteristic slow relaxation (tail current) evoked by a voltage step from  $-28$  to  $-48$  mV (**Fig. 1**). As expected<sup>26</sup>, this relaxation was abolished by the M-channel blocker XE991. The  $I_M$  amplitude in CA1 neurons of mutants was markedly reduced compared to mutants on dox ( $17.12 \pm 6.41$  pA,  $n = 16$ , compared to  $70.61 \pm 6.03$  pA,  $n = 11$ , respectively; **Fig. 1**).

### Epilepsy phenotype

Most male mutants (~60%, or 51 of 86) showed frequent ‘stargazer’-like dorsal head and neck extensions, which were likely indicative of partial seizures (**Fig. 2a** and **Supplementary Video 1** online). Other signs of seizures were asymmetrical extensor spasms of the forelimbs. These were occasionally followed by spontaneous generalized tonic-

clonic seizures lasting around 15–30 s (**Fig. 2b** and **Supplementary Video 2** online; ~5% of male mutants, or 3 out of 64). In contrast, no spontaneous seizure activity was observed in any of the female mutants ( $n > 100$ ), controls ( $n > 200$ ) or male mutant-on-dox mice ( $n > 100$ ). This gender difference in the occurrence of spontaneous seizures was probably related to the mosaic expression of hQ2-G279S in females.

We combined infrared video and telemetric electrocorticogram (ECoG) recordings to monitor behavior and spontaneous electrographic activity in freely moving male mutants ( $n = 8$ ) and male controls ( $n = 11$ ). These recordings were done during the day and night phases of at least three randomly selected days within a three-week period. When control mice were exploring (a new cage, for example), their ECoG was dominated by highly synchronous cortical activity in the theta frequency range (6–10 Hz), which typically lasted from several seconds to minutes (**Fig. 2c**). Mutant mice (five of eight), by contrast, displayed frequent sharp-wave activity, often associated with asymmetrical short-limb extensions or with head bobs (as described above), during similar periods of exploration (**Fig. 2d** and **Supplementary Video 3** online). This activity was most likely indicative of partial seizures without secondary generalization. The frequency

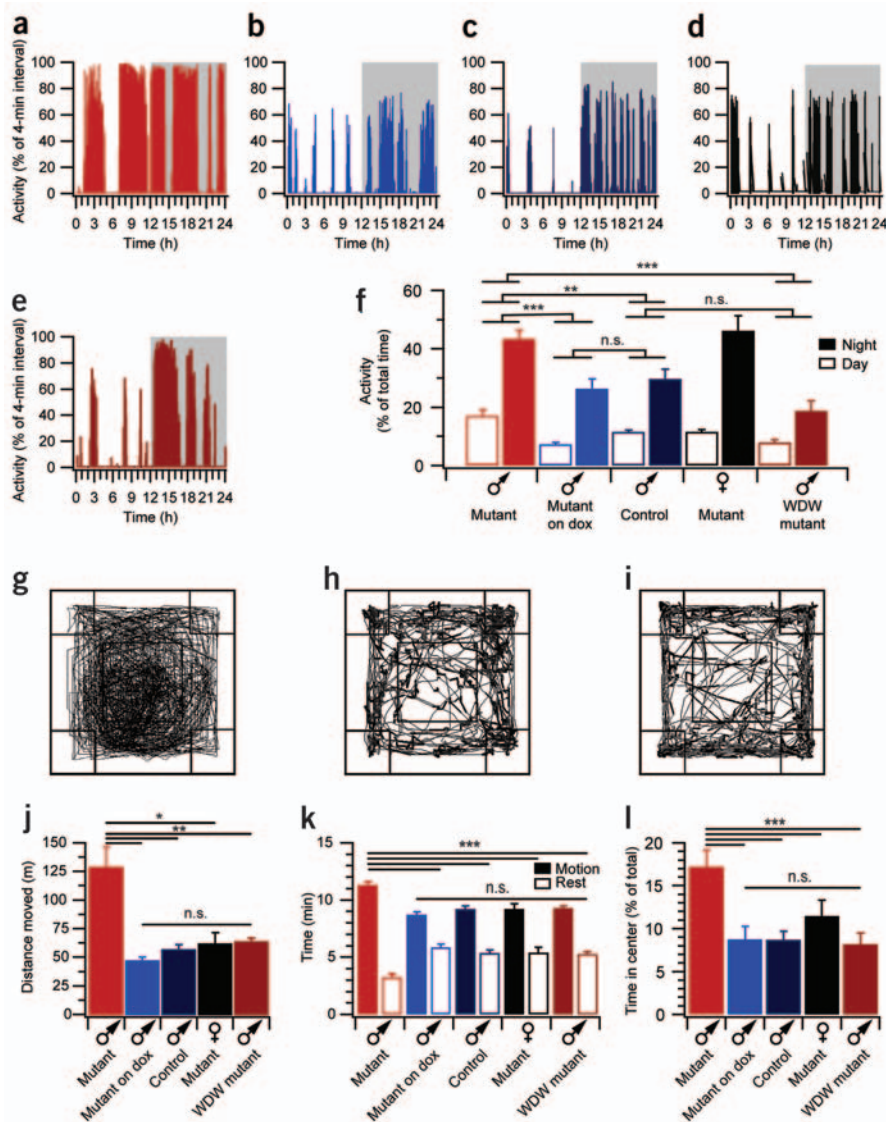


**Figure 3** Home-cage and open-field activity. (**a–e**) Analysis of home cage activity. Sample activity patterns during a 24-h period consisting of 12 h daylight and 12 h darkness (gray background) for a male mutant (**a**), mutant on dox (**b**), control (**c**), female mutant (**d**) and male WDW mutant (**e**;  $n = 10$  in each group). (**f**) Summary statistics for the mean activity of the mice in their home cages during 12-h intervals as recorded for the respective groups shown in **a–e**. (**g–i**) Open field behavior of the five groups of mice analyzed in **a–e**. Sample path recordings of a hyperactive male mutant (**g**), a mutant-on-dox (**h**) and a WDW mutant male (**i**) during a 15-min period. (**j–l**) Summary statistics for the open-field behavior during a 15-min test period with respect to the distance moved (**j**), motion and rest times (**k**) and time in center (**l**). Error bars, s.e.m. \*,  $P < 0.05$ ; \*\*,  $P < 0.01$ ; \*\*\*,  $P < 0.001$  (two-way repeated-measures ANOVA).

of each sex) showed a ~1.5-fold increase in cage activity as compared to male controls ( $n = 10$ ) or to male mutant-on-dox mice ( $n = 10$ ; **Fig. 3**). The differences were most pronounced during the dark periods.

In the open-field test, male mutants showed marked hyperactivity, but female mutants did not (**Fig. 3** and **Supplementary Video 4** online). Mutant males failed to habituate to the testing environment in 15 min, and during this period covered more than twice the distance as their control-male or mutant-female littermates. The average resting times of mutant males were significantly shorter than those of controls  $P < 0.001$  (**Fig. 3**). Tracings of running paths showed that male mutants did not have a preference for a particular area in the test arena, whereas mutant-on-dox mice clearly avoided crossing the central part of the arena (**Fig. 3**).

of the observed high-amplitude sharp waves in mutants was usually 0.5–2 Hz, and the episodes, lasting ~5–30 s, occurred several times an hour during wakefulness. Over a 72-h observation period, we observed in three of these five mutant mice up to 20 episodes per day of stereotyped slow high-amplitude spike-and-wave activity at frequencies below 2 Hz, each lasting from seconds to minutes (**Fig. 2e**). This activity was usually accompanied by rhythmic movements of the head or limbs. The seizure activity in the ECoG was self-limiting and did not lead to status epilepticus. The remaining three mutants showed several isolated high-amplitude paroxysmal sharp waves per hour, without any signs of abnormal behavior.

### Behavioral hyperactivity

Most male mutants (~80%,  $n = 79$ ) showed conspicuous behavioral changes, including frequent episodes of increased locomotor activity (several times per hour during wakefulness) with stereotyped circling and ‘tail catching’. This hyperactive behavior was most pronounced when the mutant males were placed in a new environment (for example, a new cage). In contrast, female mutants rarely showed such abnormal hyperactivity (only 5 out of 146 did so). We monitored the activity of individual mice in their home cage for at least three consecutive days (12-h light/12-h dark cycle; **Fig. 3**). Mice from all groups showed a normal circadian rhythm. However, both male and female mutants ( $n = 10$

### Identification of a critical period for phenotype development

Nissl-stained coronal hippocampal sections showed dispersion of neurons in the CA1 field of male mutants ( $n = 15$ ), but not in the CA1 field of controls ( $n = 10$ ), mutants on dox ( $n = 7$ ) or female mutants ( $n = 5$ ; **Fig. 4**). A slight reduction in staining and a pronounced loss of Timm-stained mossy fiber terminals were detected in the infrapyramidal layer of CA3 in mutant males ( $n = 5$ ) as compared to controls ( $n = 10$ ), mutants on dox ( $n = 8$ ) or female mutants ( $n = 3$ ; **Fig. 4**). The data indicate significant hippocampal pathology in brains of male mutants. In contrast to rodent models of drug-induced status epilepticus<sup>27,28</sup>, we did not find mossy-fiber sprouting in the infrapyramidal layer or in the stratum oriens of CA3. Given the age dependence of human BFNC, of seizure susceptibility and of seizure-induced cell loss in pharmacological epilepsy models<sup>29</sup>, we hypothesized that the consequences of M-current deficiency might differ between developmental periods. We used the Tet-Off system (**Fig. 1**) to switch off transgene expression (and thus  $I_M$  deficiency) during defined periods by adding doxycycline to the drinking water (**Supplementary Fig. 2** online). We found that the first weeks of life represented a critical period during which the dominant-negative transgene led to the described morphological changes in hippocampus, to behavioral hyperactivity and to frequent seizures (**Supplementary Fig. 2** online). Whereas newborn mutant males (on

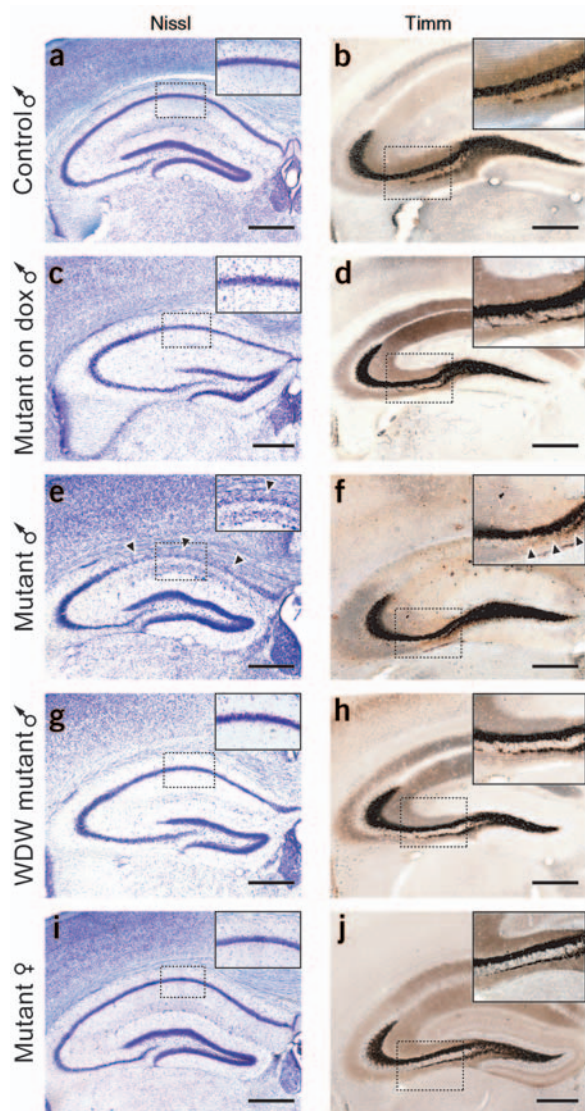


**Figure 4** Morphological analyses in hippocampus. (a–j) Representative coronal Nissl- (left column) or Timm-stained (right column) sections through the hippocampal region of male control (a,b), mutant-on-dox (c,d), mutant (e,f), WDW mutant (g,h) and female mutant (i,j) mice. The insets illustrate a magnification of the area marked by a dotted rectangle. Arrows in e and f highlight morphological changes, including cell dispersion and apparent cell loss (e) and attenuation of Timm-stain intensity of mossy fiber terminals in the infrapyramidal layer of CA3 (f). These changes were seen exclusively in sections from male mutants. Scale bar, 500  $\mu$ m

We therefore examined WDW mutants ( $n = 7$ ) for the possible presence of ECoG changes due to M-channel suppression. The ECoGs recorded for all seven mice showed periods of abnormal activity consisting of frequent (several times per hour) stereotyped bursts of spike-wave (Fig. 2f) or wave activity at 3–6 Hz, which typically lasted 2–60 s. Similar to ECoG patterns of partial seizures in male mutants, recordings from WDW mutants revealed stereotypic bursts of slow spike-wave activity followed by suppression of ECoG activity and low amplitudes (Fig. 2g). These ECoG patterns occurred several times per day, were of lower amplitude than those of mutants and were often accompanied by rhythmic head bobs or asymmetric extensor spasms of the forelimbs. Our data thus show that WDW mutants had abnormally increased cortical excitability despite having normal hippocampal morphology.

#### Biophysical properties of CA1 pyramidal neurons

To investigate the consequences of M-current suppression on single neurons, we analyzed the biophysical properties of CA1 pyramidal neurons in hippocampal slices from male controls, mutants, mutants on dox and WDW mutants. We did not observe any statistically significant difference between CA1 neurons from the four groups of mice in action-potential parameters such as threshold, amplitude, maximal-rise slope, maximal-decay slope, half-width or 90–10% decay time (data not shown). There were also no significant differences between the resting membrane potentials of CA1 pyramidal cells at baseline conditions (see **Supplementary Data** online), although the M current was strongly reduced in both groups of mutants that expressed the dominant-negative subunit (mutants and WDW mutants) (Fig. 1). In contrast, the mean input resistance ( $R_{\text{input}}$ ) at subthreshold depolarized potentials (between  $-58$  and  $-68$  mV; Methods and **Supplementary Data** and **Supplementary Fig. 5** online) was higher in cells from mutants than in cells from controls or from mutants on dox.

We studied cellular excitability and spike-frequency adaptation by injecting 500-ms depolarizing-current pulses of different intensities into the CA1 neurons (Fig. 5). Cells from mutant and WDW-mutant mice produced significantly more action potentials per pulse and showed a markedly weaker spike-frequency adaptation than cells from controls or from mutants on dox (Fig. 5). Furthermore, the M-channel blocker XE991 had a significantly stronger effect on spike number and spike-frequency adaptation in control or mutant-on-dox cells than in cells from mutants or WDW mutants (Fig. 5). Thus, M-channel deficiency was correlated with markedly increased neuronal excitability. This hyperexcitability was also observed in neurons from WDW mutants without morphological changes (Fig. 5), indicating that it must have been independent of such changes.

Next, we tested the contribution of KCNQ channels to the mAHP. CA1 pyramidal neurons from mutants on dox and controls showed a robust mAHP following a train of four spikes evoked by injection of a 50-ms depolarizing current pulse into the cell (Fig. 6). Application of 10  $\mu$ M XE991 reduced the mAHP amplitude by  $\sim 75\%$ . Similar current pulses elicited hardly any detectable mAHPs in mutant and WDW mutant cells, and application of XE991 had little or no effect. Comparable results were obtained for mAHPs following one to five

water) had no obvious structural changes in the hippocampus, post-natal day 7 (P7) mice showed a slight dispersion of the CA1 pyramidal cell layer, which progressed in P14 and P21 mutants (data not shown). By adding doxycycline to the drinking water of the mothers at P0 and maintaining treatment for one, two or three weeks, we obtained adult male ‘water-dox-water’ (WDW) mutant mice with normal hippocampal morphology (Fig. 4). The absence of morphological alterations was not due to attenuated transgene expression in WDW mutants, because hQ2-G279S expression levels were comparable to those of mutants (Fig. 1). In addition, WDW mutants and male mutants showed a similar attenuation of  $I_M$  in CA1 pyramidal neurons (Fig. 1;  $n = 5$ ). Because adult WDW mutants were M-channel deficient and had normal hippocampi, we used these mice as a fifth group to discriminate direct functional effects of the dominant-negative transgene from possible secondary changes caused by morphological alterations.

WDW mutants behaved like controls and showed no overt abnormalities in home-cage and open-field activity (Fig. 3). These findings indicate that behavioral hyperactivity only developed when M-channel deficiency was induced during a critical period in the first postnatal weeks. The behaviors that frequently accompanied partial or generalized seizures in male mutants were not seen in WDW mutants ( $n = 30$ ).

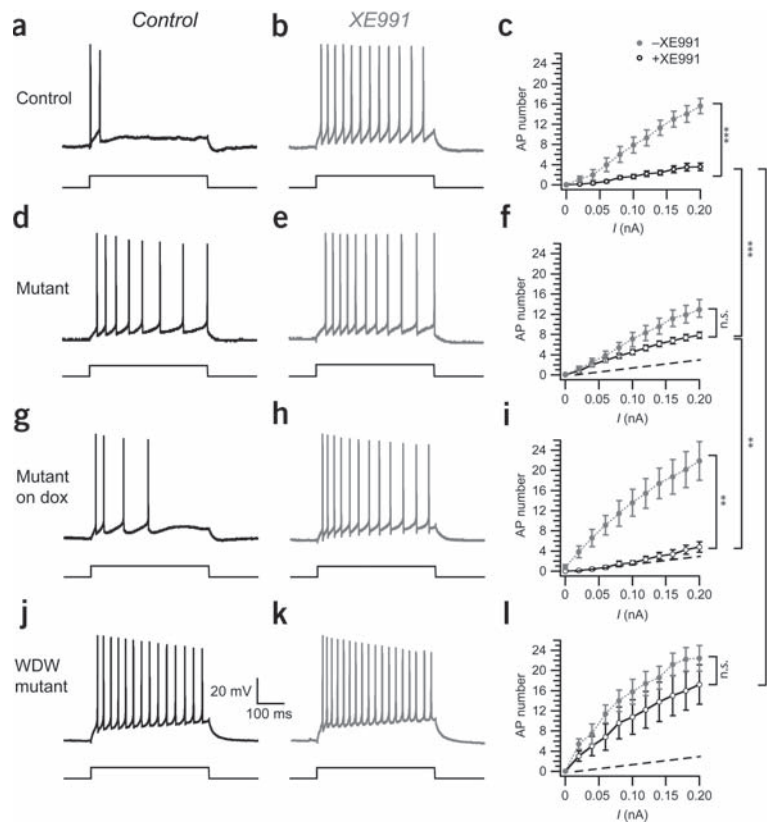


**Figure 5** Comparison of spike-frequency adaptation in CA1 pyramidal neurons. Spike trains were evoked by injecting 500-ms depolarizing current pulses of different intensities (0–0.2 nA) into the cell from a holding level of  $-58$  mV before (black) and after (gray) application of XE991. Left panels show representative recordings in normal extracellular medium (**a,d,g,j**) and middle panels after application of  $10 \mu\text{M}$  XE991 for 10 min (**b,e,h,k**). Spike-frequency adaptation was reduced in mutant (**d**;  $n = 31$  cells from ten mice) and WDW mutant mice (**j**;  $n = 5$ , two mice) in comparison to control (**a**;  $n = 14$ ; five mice) or mutant-on-dox mice (**g**;  $n = 9$ , three mice). XE991 was less effective in mutants (**e**;  $n = 13$ , seven mice) and WDW mutants (**k**;  $n = 5$ , two mice) than in the two other groups (**b,h**;  $n = 7$ , four mice;  $n = 7$ , three mice, respectively). Summary diagrams (right column) compare the number of action potentials before (black) and after (gray) application of XE991 in controls (**c**), mutants (**f**), mutants on dox (**i**) and WDW mutants (**l**). The dashed line shows the number of action potentials observed in controls. Error bars, s.e.m. \*,  $P < 0.05$ ; \*\*,  $P < 0.01$ ; \*\*\*,  $P < 0.001$  (two-way repeated measures ANOVA).

action potentials (Fig. 6). These results demonstrate that the dominant-negative transgene suppressed the mAHP in CA1 pyramidal neurons from mutants and WDW mutants, thus mimicking and occluding the blockade of M channels with XE991. Furthermore, recordings from cells from female mutants yielded markedly varying mAHP amplitudes and spike-frequency adaptation of CA1 neurons from the same mouse (data not shown), which is in accordance with the observed X-chromosomal inheritance of the dominant-negative transgene.

To rule out that the reduction of the mAHP in mutant CA1 neurons might be due to a reduction in the contribution from small-conductance  $\text{Ca}^{2+}$ -activated  $\text{K}^{+}$  (SK) channels<sup>30</sup>, we recorded the apamin-sensitive  $I_{\text{AHP}}$  from mutant and mutant-on-dox CA1 pyramidal cells. We found that there was no significant difference in apamin-sensitive  $I_{\text{AHP}}$  amplitude between these two groups ( $152.25 \pm 30.10$  pA,  $n = 3$ , for mutants on dox and  $212.63 \pm 50.83$  pA,  $n = 4$ , for mutants;  $P = 0.35$ ; data not shown), confirming that the attenuation of the mAHP in mutant CA1 pyramidal cells was due to  $I_{\text{M}}$  suppression.

### Intrinsic resonance properties

M currents activate at membrane potentials that are more negative than the action-potential threshold and are therefore well suited to modulate intrinsic membrane properties and to produce resonance at subthreshold potentials. It was recently reported that M channels produce resonance in the theta frequency range at depolarized subthreshold potentials (called ‘M-resonance’) in rat hippocampal pyramidal neurons<sup>26</sup>. We therefore compared the electrical-resonance behavior of CA1 pyramidal neurons from male mutants, mutants on dox and WDW mutants by applying the impedance amplitude profile (ZAP) method (Fig. 7; Methods)<sup>26,31</sup>. Injections of oscillating currents of varying frequencies into mutant-on-dox neurons induced membrane voltage oscillations with peak amplitudes at 3–5 Hz (Fig. 7). A reso-

nance peak in the impedance plots occurred at  $3.7 \pm 0.4$  Hz with a Q factor of  $1.7 \pm 0.1$  ( $n = 8$ ; Fig. 7), indicating a prominent resonance at theta frequencies. Such a resonance peak has also been observed in rat hippocampal neurons<sup>26,32,33</sup>. Application of the same ZAP protocol to mutant CA1 pyramidal neurons produced much larger voltage deflections (in accordance with the increased  $R_{\text{input}}$ ; see above), thus triggering spikes that prevented subthreshold resonance analysis. We therefore reduced the ZAP current intensity to a level that produced the same peak-to-peak amplitude as in mutant-on-dox cells. This procedure revealed that the neurons from both mutants and WDW mutants lacked a clear resonance peak (Fig. 7). Instead, their peak voltage response occurred close to the lowest frequency tested ( $1.4 \pm 0.4$  Hz for mutants,  $0.75 \pm 0.25$  Hz for WDW mutants; Fig. 7) and with a Q factor close to 1.0 ( $1.1 \pm 0.1$ ,  $n = 12$  for mutants,  $1.0 \pm 0.0$  for WDW mutants; Fig. 7), indicating lack of resonance<sup>26,34</sup>.

To test whether the attenuation of M-resonance in mutant and WDW-mutant cells might be due to a reduction in persistent  $\text{Na}^{+}$  current ( $I_{\text{NaP}}$ )<sup>26</sup>, we compared the M-resonance in mutant-on-dox and mutant CA1 cells after blocking  $I_{\text{NaP}}$  with tetrodotoxin (TTX). In the presence of TTX, injection of ZAP current into CA1 pyramidal neurons from mutants on dox evoked typical resonating voltage responses at a membrane potential of  $-48$  mV<sup>26</sup> (Q factor,  $1.28 \pm 0.13$ , resonance frequency,  $3.94 \pm 0.34$  Hz,  $n = 7$ ). However, cells from mutant mice showed essentially no resonance under the same testing conditions (Q factor,  $1.01 \pm 0.01$ , resonance frequency,  $1.05 \pm 0.21$  Hz,  $n = 10$ ). Subsequent application of XE991 blocked the resonance in mutant-on-dox cells ( $n = 5$ ) but had little effect on mutant cells ( $n = 9$ ; Supplementary Fig. 3 online).

The specificity of our transgenic approach leading to the selective attenuation of M-resonance at depolarized potentials was further investigated in mutant-on-dox and mutant cells. No differences were found in resonance properties at hyperpolarized potentials. Whereas M channels are closed at these voltages, H-channels are active and generate the so-called ‘H-resonance’<sup>26</sup> (Supplementary Fig. 4 online).

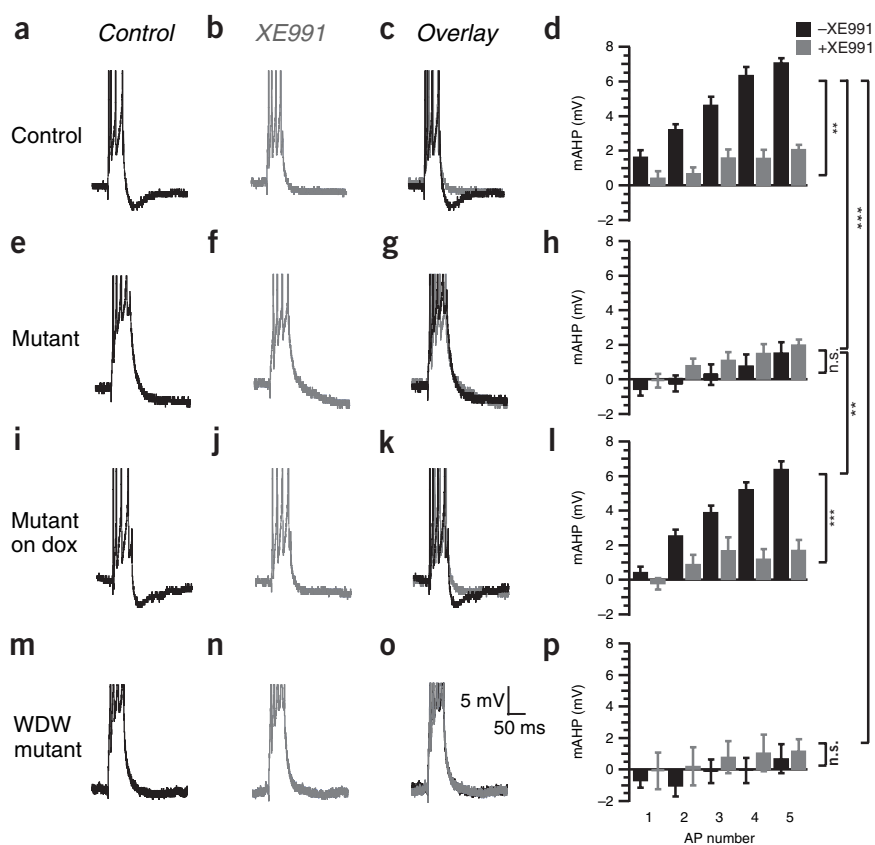


**Figure 6** Comparison of the medium afterhyperpolarizations (mAHPs) following spike trains in CA1 pyramidal cells. Whole-cell recordings from hippocampal slices. Representative recordings of the mAHP recorded in normal medium (**a,e,i,m**) and after application of 10 μM XE991 for 10 min (**b,f,j,n**). To the right (**c,g,k,o**), both traces are shown superimposed. mAHP was small in mutant mice (**e**;  $n = 26$  cells from ten mice) and WDW mutant mice (**m**;  $n = 5$ , two mice) compared to control (**a**;  $n = 9$ , seven mice) or mutant-on-dox (**i**;  $n = 9$ , three mice) mice. XE991 had little or no effect in mutant mice (**f,g**;  $n = 15$ , nine mice) and WDW mutant mice (**n,o**;  $n = 5$ , two mice) as compared to the two other groups (**b,c**;  $n = 6$ , four mice, **j,k**;  $n = 7$ , three mice). Summary diagrams compare mAHP peak amplitudes following one to five action potentials before (black columns) and after (gray columns) application of XE991 in controls (**d**), mutants (**h**), mutants on dox (**l**) and WDW mutants (**p**). XE991 significantly reduced mAHPs evoked by two to five action potentials in controls (**d**) and mutants on dox (**l**) but not in mutants (**h**) and WDW mutants (**p**). Action potentials are shown truncated for clarity. Error bars, s.e.m. \*,  $P < 0.05$ ; \*\*,  $P < 0.01$ ; \*\*\*,  $P < 0.001$  (two-way repeated measures ANOVA).

the medium afterhyperpolarization (mAHP) and for early spike-frequency adaptation in hippocampal pyramidal neurons, and it helps to clarify the roles of these channels in relation to the neuronal resting potential and input

resistance. Our results also demonstrate that KCNQ/M channels are essential for the characteristic subthreshold theta frequency resonance of hippocampal pyramidal cells<sup>26</sup>—a functional property that is likely to be important for hippocampal learning and memory<sup>36</sup>. The data further indicate that suppression of  $I_M$  in adult mice causes impairment of hippocampus-dependent memory, whereas  $I_M$  suppression during early neonatal development results in morphological changes in the brain, profound hyperactivity and frequent spontaneous seizure activity. The latter condition is reminiscent of an inherited form of human epilepsy (BFNC) caused by *KCNQ2/3* gene mutations.

By using the Tet-Off system, we controlled temporal expression of the dominant-negative hQ2-G279S. *In vitro*, hQ2-G279S interfered with the expression of functional M channels assembled from mouse KCNQ2 and/or KCNQ3 subunits. It is likely that hQ2-G279S exerted its dominant-negative effect on M-channel activity by replacing KCNQ2 and/or KCNQ3 subunits in heteromultimeric M channels. A similar mechanism was probably responsible for the marked reduction in the native XE991-sensitive M-current amplitude in mutant hQ2-G279S-expressing CA1 pyramidal neurons. The small residual  $I_M$  detected in our voltage-clamp experiments in mutant neurons might have been mediated by KCNQ5 subunits, which constitute a likely component of neuronal M channels<sup>15,37</sup> but do not co-assemble with hQ2-G279S subunits<sup>37</sup>. Our data therefore indicate that the major M-channel subunits in CA1 pyramidal neurons are KCNQ2 and/or KCNQ3.

Two different types of  $K^+$  channels have been suggested to underlie the mAHP and the spike-frequency adaptation in CA1 pyramidal neurons, namely the  $Ca^{2+}$ -activated SK channels<sup>38–40</sup> and the M channels<sup>4,18,41</sup>. We investigated the contribution of M channels to mAHP and early spike-frequency adaptation in current-clamp recordings from CA1 pyramidal neurons. Mutant cells showed much smaller mAHPs, reduced early spike-frequency adaptation and less XE991 sensitivity, and there was no

### Morris water maze performance

The performance of mutant mice in hippocampus-dependent spatial learning and memory tests may be affected by altered excitability of hippocampal neurons. We used the Morris water maze<sup>35</sup> to test hippocampus-dependent learning and memory performance in male WDW mutants and female mutants. Male mutants had difficulty swimming, whereas male WDW and female mutants showed normal swimming speed and thigmotaxis (swimming close to the pool wall) compared to controls (data not shown).

All mice tested (male WDW, female mutants and mutants on dox of either gender) learned the cued version of the test (with a visible platform) equally well. Additionally, when the platform was submerged (hidden), all animal groups showed a similar decrease in escape latency and path-length position during a three-day acquisition period (data not shown), which is typical of wild-type mice in the Morris water maze test. However, in the probe trial, which had no platform and was performed on the third day to test whether the mice remembered the platform position, both male WDW mutants ( $n = 11$ ) and female mutants ( $n = 9$ ) performed poorly. When searching for the missing platform, these mice spent nearly equal times in the four quadrants (**Fig. 8**). In contrast, mutant-on-dox mice ( $n = 12$  females and 10 males) spent more than 42% of the test period in the target quadrant, indicating a clear preference for the correct position (**Fig. 8**).

### DISCUSSION

This study demonstrates that the expression of a dominant-negative KCNQ2 subunit in transgenic mice is an effective method for suppressing  $I_M$  in the mammalian brain. Furthermore, it provides the first direct molecular evidence of functional roles for KCNQ/M channels in the central nervous system at cellular, network and behavioral levels. It shows that KCNQ/M channels are essential for excitability control, for

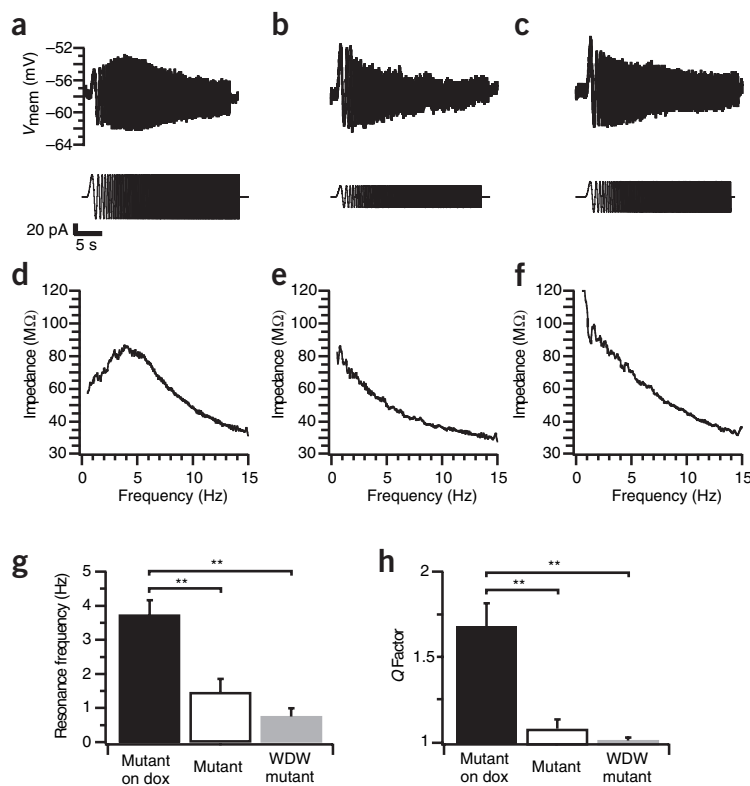


**Figure 7** Resonance behavior of CA1 pyramidal neurons at depolarized membrane potentials (M-resonance). (a–c) Typical membrane-potential response to a ZAP current injection in cells from mutants on dox (a;  $n = 8$  cells from three mice), mutants (b;  $n = 12$ , five mice) and WDW mutants (c;  $n = 5$ , two mice). (d–f) Impedance plotted as a function of input frequency calculated from the data shown in a–c. Unlike mutant (e) and WDW-mutant (f) cells, mutant on dox (d) cells showed a clear resonance peak near 4 Hz. (g) The peak impedance occurred around 4 Hz in cells from mutants on dox, whereas cells from mutants and WDW mutants showed peak impedances close to 1 Hz. (h) As indicated by the  $Q$  factors, the strength of the observed resonance was higher in mutant-on-dox than in mutant and WDW mutant cells. Error bars, s.e.m. \*\*,  $P < 0.01$  ( $t$ -test).

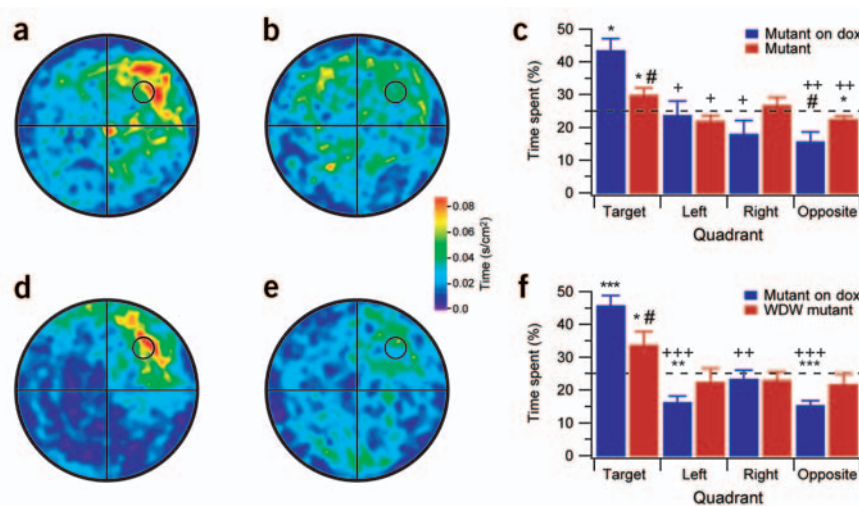
for synaptic input within the theta frequency range<sup>26,32,33</sup>. The CA1 field is a prominent current generator, producing network theta oscillations<sup>36</sup>, which are typical of the hippocampal EEG in humans and in behaving animals<sup>36,42–44</sup>. These oscillations are proposed to be of central importance to hippocampus-dependent spatial learning and memory<sup>36</sup>.

Adult male mutants (in which  $I_M$  was suppressed throughout life) had frequent, spontaneous and predominantly partial seizures. The dispersion of the CA1 pyramidal-cell layer seen in these mice was comparable to that found in rodent models of pharmacologically induced status epilepticus<sup>27,28</sup>. Similar changes were also observed for human temporal lobe epilepsy<sup>45</sup>. Timm staining of hippocampal mossy fibers showed a loss of mossy fiber terminals in the infrapyramidal layer of CA3 but no mossy fiber sprouting. We used the Tet-Off system to restrict hQ2-G279S expression to different periods in pre-and/or postnatal development by giving doxycycline during different periods. The results showed that the mutant mice receiving doxycycline during the first weeks of life (WDW mutants) had morphologically normal brains. Our results indicate that the severe-epilepsy phenotype, as well as the frequent behavioral seizures and marked hyperactivity, were due to developmental defects caused by  $I_M$  suppression within the first postnatal weeks rather than to reduced

significant change in apamin-sensitive  $I_{AHP}$  mediated by SK channels. Our results thus demonstrate that M channels have a major role in the generation of mAHP and in early spike-frequency adaptation in CA1 pyramidal neurons<sup>4,18,19</sup>. Furthermore, M channels are likely to be important in regulating electrical responsiveness at subthreshold levels. Although the resting membrane potential of mutant CA1 pyramidal neurons was not altered, the mean input resistance in the subthreshold membrane-potential range was higher in mutants than in controls. In this membrane-potential range, CA1 pyramidal neurons from doxycycline-treated control mice showed prominent intrinsic resonance at theta frequencies (~4 Hz at 30 °C), but mutant CA1 neurons selectively lacked this resonance and behaved as if they were dominated by passive membrane properties. The results are in agreement with previous electrophysiological and pharmacological studies of rat CA1 pyramidal neurons, which suggest that M channels are essential to the characteristic preference of CA1 pyramidal neurons

for synaptic input within the theta frequency range<sup>26,32,33</sup>. The CA1 field is a prominent current generator, producing network theta oscillations<sup>36</sup>, which are typical of the hippocampal EEG in humans and in behaving animals<sup>36,42–44</sup>. These oscillations are proposed to be of central importance to hippocampus-dependent spatial learning and memory<sup>36</sup>.

**Figure 8** Morris water-maze test. (a,b,d,e) Spatial histograms of the mice's positions during the probe trial of the Morris water maze test: female mutants on dox (a;  $n = 12$ ), female mutants (b;  $n = 9$ ), male mutants on dox (d;  $n = 11$ ) and WDW mutants (e;  $n = 11$ ). Color scale as given on the right of the histograms. (c,f) Mean time spent in the quadrants during a 60-s probe trial. Female mutants spent significantly less time in the target quadrant than female mutants on dox (c). Male WDW mutants also had a strongly decreased preference for the target quadrant compared to male mutants on dox (f). Error bars, s.e.m. \*,  $P < 0.05$  (Wilcoxon signed rank test); #,  $P < 0.05$ ; ###,  $P < 0.001$  (Mann-Whitney test); +,  $P < 0.05$ ; ++,  $P < 0.01$  (Wilcoxon test).



$I_M$  in adulthood (Supplementary Fig. 2 online); this was indicated by the comparable levels of *hQ2-G279S* mRNA in mutants and WDW mutants, and the similar degree of  $I_M$  suppression in these groups (Fig. 1).

Electrophysiological analysis of CA1 pyramidal neurons from WDW mutants underscored the importance of M channels in tuning cellular responses to excitatory input. In WDW mutant CA1 neurons,  $I_M$  and mAHP amplitudes were severely attenuated, excitability was markedly increased and the intrinsic theta resonance to oscillating current inputs was lost. A comparison of the results obtained from mutants and WDW mutants indicates that the measured responses to excitatory inputs were affected in a cell-autonomous manner by suppressing  $I_M$  and not by altering hippocampal morphology. By contrast, the overt hyperactivity and frequent partial seizures with high-amplitude ECoG activity in male mutants were linked to the abnormal morphology of mutant brains. Consequently, WDW mutants did not show overt hyperactivity and partial seizures were also far less frequent. Still, WDW mutants showed abnormally synchronized cortical network patterns. However, as WDW mutants, unlike male mutants, did not show brain morphology changes, it is likely that the changes in cortical ECoG activity in WDW mutants reflect an important role for M channels in the generation of normal network activity. This is supported by the profoundly impaired spatial-memory performance of male WDW mutants and female mutants in the Morris water maze.

The results of the alternating doxycycline treatment showed that M-channel deficiency during the first weeks of life triggers persistent changes in morphology and/or synaptic organization (WD mutants; Supplementary Fig. 2 online). In this context, it is important to note that the neonatal brain is particularly prone to seizures<sup>29</sup>. For example, seizure-like events in hippocampal slices from neonatal rats were inducible by 8.5 mM extracellular  $K^+$  only in a narrow time window between P7 and P16, peaking around P11 (ref. 46). High extracellular  $[K^+]$  reduces  $K^+$  currents, thus mimicking a partial block of  $K^+$  channels, including M channels. Notably, the developmental time windows of  $K^+$ -induced seizure susceptibility and those of *hQ2-G279S*-induced hippocampal pathology and behavioral abnormalities are quite similar.

Thus, it seems that the first two weeks of postnatal brain development represent a critical period for phenotype development in these mutant mice. During this period, GABA, the major inhibitory neurotransmitter in adult brain, provides the main excitatory drive to immature hippocampal neurons, and inhibition in neonatal circuits appears to be mainly mediated by presynaptic inhibition through control of neurotransmitter release<sup>47</sup>. M channels, which are localized to axon initial segments, axons and synaptic terminals<sup>16,17</sup>, may be involved in the control of neurotransmitter release<sup>48,49</sup>. Attenuation of  $I_M$  in the mutants might therefore alter transmitter release and, in this way, affect presynaptic control of inhibition. Whether this mechanism underlies perturbed neuronal migration and results in altered synaptic organization needs to be investigated.

Although the prion protein promoter-driven transgene expression in our double-transgenic mouse line was limited to the nervous system, it is not restricted to principal neurons in the hippocampus. The presently available data and methodological approach do not allow us to determine the contribution of specific neuron populations (for example, glutamatergic or GABAergic neurons) to the observed abnormal network patterns. Many gene mutations that are linked to epilepsy syndromes are known to interfere with the delicate balance between excitation and inhibition by attenuating inhibition<sup>50</sup>. Thus, it is possible that reduced inhibition, for example due to altered interneuron activity or neurotransmitter release, contributes to the epilepsy phenotype in our mutant mice.

Regardless of these possible explanations, the results presented here provide the first direct evidence of functional roles for M channels in the central nervous system at the cellular, network and behavioral levels. Our transgenic strategy offers a promising approach to investigating the

physiological and pathophysiological roles of M channels in cognitive functions, neuroprotection and epilepsy.

## METHODS

Methods for testing the dominant-negative *hQ2-G279S* construct by heterologous expression in *Xenopus laevis* oocytes and further experimental details are given in Supplementary Methods online.

**Transgene construct.** The verified *hQ2-G279S* cDNA was subcloned into pTre plasmids (Clontech). Transgenic mice carrying a HindIII-SspI TRE-*hKCNQ2-G279S* plasmid fragment were generated by pronuclear injection using standard techniques.

**Animal handling.** Double-transgenic mice received either water (for mutants) or doxycycline hydrochloride (for mutants on dox; 200  $\mu$ g/ml, Sigma) in water that was administered to mothers as early as during pregnancy. Alternative treatment schedules with the same doxycycline concentration are shown in Supplementary Figure 2 online. The experimental procedures were approved (for Hamburg) by the Ministry of Science and Public Health of the City State of Hamburg, Germany and (for Oslo) by the responsible veterinarian of the Institute of Basal Medical Sciences in accordance with the statute regulating animal experimentation of the Norwegian Ministry of Agriculture, 1996. All experimental procedures also complied with the regulations of the US National Institutes of Health and with those of the Society for Neuroscience (USA).

**Morphological analysis.** Adult mice were deeply anesthetized and perfused transcardially with phosphate-buffered saline followed by 4% paraformaldehyde for Nissl staining, or with Ringer solution followed by phosphate-buffered 1% sodium thiosulfide and 3% glutaraldehyde for Timm staining. Brains were removed and post-fixed overnight at 4 °C. Serial coronal vibratome slices (50  $\mu$ m) were mounted on glass slides and stained for Nissl substance. For Timm staining, brain slices mounted on glass slides were developed in a solution containing Arabic gum, hydroquinone, citric acid, and silver nitrate. The staining reaction was carried out in the dark at 37 °C for 30–45 min. After development, slides were rinsed with water and fixed with 1% sodium thiosulfate, dehydrated in an alcohol series and xylene, and coverslipped with Entellan (Merck).

**Slice preparation, recording and stimulation conditions.** The methods were identical to those described previously<sup>26</sup> (detailed in Supplementary Methods online). Briefly, somatic recordings were obtained from CA1 pyramidal cells in transverse hippocampal slices (400- $\mu$ m thick) from 6- to 24-week-old mice using the 'blind' method and patch pipettes filled with a solution containing (in mM): 140 KMeSO<sub>4</sub>, 10 HEPES, 10 phosphocreatine Na salt, 2 ATP Na salt, 0.4 GTP Na salt, and 2 MgCl<sub>2</sub>, giving a pipette resistance of 4–7 M $\Omega$ . The recordings were done using an Axoclamp 2A or an Axopatch 1D amplifier (Axon Instruments, Inc.) with a series resistance of 10–40 M $\Omega$ . All potentials were corrected for the liquid junction potential.

**Analysis of electrical resonance and subthreshold oscillations.** The impedance ( $Z$ )-amplitude-profile (ZAP) method was used to characterize the electrical resonance behavior of the neurons<sup>31</sup>. During whole-cell bridge current-clamp recording, a sinusoidal current with constant amplitude and linearly increasing frequency (0–15 Hz over 20 s; the ZAP current) was injected through the recording electrode, and the voltage response was recorded.

**Data acquisition and analysis.** The data were acquired using pCLAMP 7.0 (Axon Instruments) at a sampling rate of 10 kHz, were digitized, stored on video tapes (Instrutec VR-10) and measured and were plotted using pCLAMP 7.0 and Origin 5.0 (Microcal) or IgorPro4 (Wavemetrics). A two-way repeated-measures ANOVA test (Statistica 5, Statsoft) was used to compare XE991-treated and untreated cells with the same genotype (within factors: XE991 application, injected current (Fig. 5) or number of spikes (Fig. 6)). To compare cells from mice with different genotypes, the in-between factor was genotype, and the within factor represented either the injected current (Fig. 5) or the number of spikes (Fig. 6). An unpaired two-sided *t*-test (Excel, Microsoft) was used to compare resonance frequencies and *Q* values ( $\alpha = 0.05$ ).

**ECoG analysis.** Telemetric ECoG analyses were performed using implantable radio transmitters (models TA10EA-F20 or TA10ETA-F20, Data Sciences

International; see **Supplementary Methods** online for details). ECoG experiments were approved by the *Ministry of Science and Public Health* of the City State of Hamburg, Germany.

**Open-field and home-cage activity.** Open-field activity of mutant ( $n = 20$ ), mutant-on-dox ( $n = 10$ ) and control mice ( $n = 10$ ) was analyzed during the dark cycle using a protocol consisting of 5-min adaptation and a trial duration of 15 min in infrared boxes (TSE Systems). The home-cage activity of the same mice was monitored for several days with an infrared motion detector developed in-house with a sampling frequency of 1 Hz and a bin size of 4 min (<http://www.infra-e-motion.de>). Statistical analysis was performed using a two-way repeated-measures ANOVA test (Statistica 5.0, Statsoft).

**Morris water maze test.** Pre-training sessions consisting of four trials per day were performed on days one and two using a visible platform and hidden landmarks. From days three to five, the mice were trained on six trials per day to find the hidden platform. The fourth trial on day five was performed as a probe trial. Further details are given in the online supplement.

**Accession numbers.** The sequence of *mKCNQ3* was entered into the NCBI GenBank database with accession number AY118171.

*Note: Supplementary information is available on the Nature Neuroscience website.*

#### ACKNOWLEDGMENTS

We thank S.B. Prusiner, UCSF, for providing the tg(Prnp-tTA) mouse line and H. Voss for animal caretaking and execution of doxycycline application protocols. We also thank F. Morellini for help with behavioral testing and statistical analysis, S. Fehr and I. Hermans-Borgmeyer for help with *in situ* hybridizations, F. Kutschera for developing the cage activity recorder, and S. Schillemeit and C. Petterson Oksvold for technical assistance. This study was supported by grants of the German Federal Ministry of Education and Research, as a part of the National Genome Research Network (NGFN), to D.I. and O.P. Research by H.H. and J.E.S. was supported by the European Commission (Contract No. QL63-1999-00827), and by the Norwegian Research Council (NFR) Medicine & Health (MH) and Norwegian Centre of Excellence (SFF) programs.

#### COMPETING FINANCIAL INTERESTS

The authors declare that they have no competing financial interests.

Received 14 September; accepted 10 November 2004

Published online at <http://www.nature.com/natureneuroscience/>

- Brown, D.A. & Adams, P.R. Muscarinic suppression of a novel voltage-sensitive K<sup>+</sup> current in a vertebrate neurone. *Nature* **283**, 673–676 (1980).
- Brown, D.A. M-currents: an update. *Trends Neurosci.* **11**, 294–299 (1988).
- Halliwel, J.V. & Adams, P.R. Voltage-clamp analysis of muscarinic excitation in hippocampal neurons. *Brain Res.* **250**, 71–92 (1982).
- Storm, J.F. Potassium currents in hippocampal pyramidal cells. *Prog. Brain Res.* **83**, 161–187 (1990).
- Jentsch, T.J. Neuronal KCNQ potassium channels: physiology and role in disease. *Nat. Rev. Neurosci.* **1**, 21–30 (2000).
- Ryan, S.G. *et al.* Benign familial neonatal convulsions: evidence for clinical and genetic heterogeneity. *Ann. Neurol.* **29**, 469–473 (1991).
- Dedek, K., Fusco, L., Teloy, N. & Steinlein, O.K. Neonatal convulsions and epileptic encephalopathy in an Italian family with a missense mutation in the fifth transmembrane region of KCNQ2. *Epilepsy Res.* **54**, 21–27 (2003).
- Borgatti, R. *et al.* A novel mutation in KCNQ2 associated with BFNC, drug resistant epilepsy, and mental retardation. *Neurology* **63**, 57–65 (2004).
- Dedek, K. *et al.* Myokymia and neonatal epilepsy caused by a mutation in the voltage sensor of the KCNQ2 K<sup>+</sup> channel. *Proc. Natl. Acad. Sci. USA* **98**, 12272–12277 (2001).
- Marrion, N.V. Control of M-current. *Annu. Rev. Physiol.* **59**, 483–504 (1997).
- Wang, H.S. *et al.* KCNQ2 and KCNQ3 potassium channel subunits: molecular correlates of the M-channel. *Science* **282**, 1890–1893 (1998).
- Selyanko, A.A. *et al.* Inhibition of KCNQ1–4 potassium channels expressed in mammalian cells via M1 muscarinic acetylcholine receptors. *J. Physiol. (Lond.)* **522**, 349–355 (2000).
- Hadley, J.K. *et al.* Stoichiometry of expressed KCNQ2/KCNQ3 potassium channels and subunit composition of native ganglionic M channels deduced from block by tetraethylammonium. *J. Neurosci.* **23**, 5012–5019 (2003).
- Cooper, E.C. Colocalization and coassembly of two human brain M-type potassium channel subunits that are mutated in epilepsy. *Proc. Natl. Acad. Sci. USA* **97**, 4914–4919 (2000).
- Shah, M.M., Mistry, M., Marsh, S.J., Brown, D.A. & Delmas, P. Molecular correlates of the M-current in cultured rat hippocampal neurons. *J. Physiol. (Lond.)* **544**, 29–37 (2002).
- Cooper, E.C., Harrington, E., Jan, Y.N. & Jan, L.Y. M channel KCNQ2 subunits are localized to key sites for control of neuronal network oscillations and synchronization in mouse brain. *J. Neurosci.* **21**, 9529–9540 (2001).
- Devaux, J.J., Kleopa, K.A., Cooper, E.C. & Scherer, S.S. KCNQ2 is a nodal K<sup>+</sup> channel. *J. Neurosci.* **24**, 1236–1244 (2004).
- Storm, J.F. An after-hyperpolarization of medium duration in rat hippocampal pyramidal cells. *J. Physiol. (Lond.)* **409**, 171–190 (1989).
- Madison, D.V. & Nicoll, R.A. Control of the repetitive discharge of rat CA 1 pyramidal neurones in vitro. *J. Physiol. (Lond.)* **354**, 319–331 (1984).
- Malenka, R.C., Madison, D.V., Andrade, R. & Nicoll, R.A. Phorbol esters mimic some cholinergic actions in hippocampal pyramidal neurons. *J. Neurosci.* **6**, 475–480 (1986).
- Watanabe, H. *et al.* Disruption of the epilepsy KCNQ2 gene results in neural hyperexcitability. *J. Neurochem.* **75**, 28–33 (2000).
- Yang, Y. *et al.* Spontaneous deletion of epilepsy gene orthologs in a mutant mouse with a low electroconvulsive threshold. *Hum. Mol. Genet.* **12**, 975–984 (2003).
- Gossen, M. & Bujard, H. Tight control of gene expression in mammalian cells by tetracycline-responsive promoters. *Proc. Natl. Acad. Sci. USA* **89**, 5547–5551 (1992).
- Tremblay, P. *et al.* Doxycycline control of prion protein transgene expression modulates prion disease in mice. *Proc. Natl. Acad. Sci. USA* **95**, 12580–12585 (1998).
- Schroeder, B.C., Kubisch, C., Stein, V. & Jentsch, T.J. Moderate loss of function of cyclic-AMP-modulated KCNQ2/KCNQ3 K<sup>+</sup> channels causes epilepsy. *Nature* **396**, 687–690 (1998).
- Hu, H., Vervaeke, K. & Storm, J.F. Two forms of electrical resonance at theta frequencies, generated by M-current, h-current and persistent Na<sup>+</sup> current in rat hippocampal pyramidal cells. *J. Physiol. (Lond.)* **545**, 783–805 (2002).
- Nitecka, L. *et al.* Maturation of kainic acid seizure-brain damage syndrome in the rat. II. Histopathological sequelae. *Neuroscience* **13**, 1073–1094 (1984).
- Mello, L.E. *et al.* Circuit mechanisms of seizures in the pilocarpine model of chronic epilepsy: cell loss and mossy fiber sprouting. *Epilepsia* **34**, 985–995 (1993).
- Holmes, G.L. & Ben-Ari, Y. Seizures in the developing brain: perhaps not so benign after all. *Neuron* **21**, 1231–1234 (1998).
- Stocker, M., Krause, M. & Pedarzani, P. An apamin-sensitive Ca<sup>2+</sup>-activated K<sup>+</sup> current in hippocampal pyramidal neurons. *Proc. Natl. Acad. Sci. USA* **96**, 4662–4667 (1999).
- Hutcheon, B. & Yarom, Y. Resonance, oscillation and the intrinsic frequency preferences of neurons. *Trends Neurosci.* **23**, 216–222 (2000).
- Pike, F.G. *et al.* Distinct frequency preferences of different types of rat hippocampal neurons in response to oscillatory input currents. *J. Physiol. (Lond.)* **529**, 205–213 (2000).
- Leung, L.S. & Yu, H.W. Theta-frequency resonance in hippocampal CA1 neurons in vitro demonstrated by sinusoidal current injection. *J. Neurophysiol.* **79**, 1592–1596 (1998).
- Hutcheon, B., Miura, R.M. & Puil, E. Subthreshold membrane resonance in neocortical neurons. *J. Neurophysiol.* **76**, 683–697 (1996).
- Morris, R.G., Garrud, P., Rawlins, J.N. & O'Keefe, J. Place navigation impaired in rats with hippocampal lesions. *Nature* **297**, 681–683 (1982).
- Buzsáki, G. Theta oscillations in the hippocampus. *Neuron* **33**, 325–340 (2002).
- Schroeder, B.C., Hechenberger, M., Weinreich, F., Kubisch, C. & Jentsch, T.J. KCNQ5, a novel potassium channel broadly expressed in brain, mediates M-type currents. *J. Biol. Chem.* **275**, 24089–24095 (2000).
- Sah, P. Ca<sup>2+</sup>-activated K<sup>+</sup> currents in neurons: types, physiological roles and modulation. *Trends Neurosci.* **19**, 150–154 (1996).
- Vergara, C., Latorre, R., Marrion, N.V. & Adelman, J.P. Calcium-activated potassium channels. *Curr. Opin. Neurobiol.* **8**, 321–329 (1998).
- Bond, C.T. *et al.* Small conductance Ca<sup>2+</sup>-activated K<sup>+</sup> channel knock-out mice reveal the identity of calcium-dependent afterhyperpolarization currents. *J. Neurosci.* **24**, 5301–5306 (2004).
- Williamson, A. & Alger, B.E. Characterization of an early afterhyperpolarization after a brief train of action potentials in rat hippocampal neurons in vitro. *J. Neurophysiol.* **63**, 72–81 (1990).
- Raghavachari, S. *et al.* Gating of human theta oscillations by a working memory task. *J. Neurosci.* **21**, 3175–3183 (2001).
- Kahana, M.J., Seelig, D. & Madsen, J.R. Theta returns. *Curr. Opin. Neurobiol.* **11**, 739–744 (2001).
- Sarnthein, J., Petsche, H., Rappelsberger, P., Shaw, G.L. & von Stein, A. Synchronization between prefrontal and posterior association cortex during human working memory. *Proc. Natl. Acad. Sci. USA* **95**, 7092–7096 (1998).
- Blümcke, I., Thom, M. & Wiestler, O.D. Ammon's horn sclerosis: a maldevelopmental disorder associated with temporal lobe epilepsy. *Brain Pathol.* **12**, 199–211 (2002).
- Khazipov, R. *et al.* Developmental changes in GABAergic actions and seizure susceptibility in the rat hippocampus. *Eur. J. Neurosci.* **19**, 590–600 (2004).
- Ben-Ari, Y. Excitatory actions of GABA during development: the nature of the nurture. *Nat. Rev. Neurosci.* **3**, 728–739 (2002).
- Lechner, S.G., Mayer, M. & Boehm, S. Activation of M1 muscarinic receptors triggers transmitter release from rat sympathetic neurons through an inhibition of M-type K<sup>+</sup> channels. *J. Physiol. (Lond.)* **553**, 789–802 (2003).
- Martire, M. *et al.* M channels containing KCNQ2 subunits modulate norepinephrine, aspartate, and GABA release from hippocampal nerve terminals. *J. Neurosci.* **24**, 592–597 (2004).
- Noebels, J.L. The biology of epilepsy genes. *Annu. Rev. Neurosci.* **26**, 599–625 (2003).